Applied Catalysis B: Environmental 89 (2009) 33–40

Contents lists available at ScienceDirect

Applied Catalysis B: Environmental

journal homepage: www.elsevier.com/locate/apcatb

The effect of sulphation on the catalytic activity of CoO_x/ZrO_2 for NO reduction with NH_3 in the presence of O_2

Daniela Pietrogiacomi [a,*], Alessandro Magliano [a], Paolo Ciambelli [b], Diana Sannino [b], Maria Cristina Campa [c], Valerio Indovina [a]

[a] Dipartimento di Chimica, Università di Roma "La Sapienza", Piazzale Aldo Moro 5, 00185 Roma, Italy
[b] Dipartimento di Ingegneria Chimica e Alimentare, Università di Salerno, via Ponte Don Melillo, 84084 Fisciano (SA), Italy
[c] Sezione "MICE" dell'Istituto I.S.C. (CNR), c/o Dipartimento di Chimica, Università di Roma "La Sapienza", Piazzale Aldo Moro 5, 00185 Roma, Italy

ARTICLE INFO

Article history:
Received 12 September 2008
Received in revised form 10 November 2008
Accepted 14 November 2008
Available online 24 November 2008

Keywords:
Selective catalytic reduction
NO reduction
Sulphated-ZrO_2
Supported cobalt oxide

ABSTRACT

Selective catalytic reduction (SCR) of NO with NH_3 in the presence of O_2, and NH_3 oxidation with O_2 ($NH_3 + O_2$) were studied on CoO_x/ZrO_2 and sulphated-CoO_x/ZrO_2 catalysts. Monoclinic CoO_x/ZrO_2 (Co/Z_m) containing 2.0 or 4.6 Co-atoms nm^{-2} were prepared by dry impregnation of monoclinic ZrO_2 (Z_m) with $Co(CH_3COO)_2$ aqueous solutions. Three sulphated catalysts, all having roughly the same surface density of cobalt (2 Co-atoms nm^{-2}) were prepared by (i) exposure of Co/Z_m to a gaseous stream $SO_2 + O_2$ (Co/Z_mS_g), (ii) impregnation of Z_m with $CoSO_4$ aqueous solution (CoS/Z_m), and (iii) impregnation of $Zr(OH)_4$ with $CoSO_4$ aqueous solution (CoS/Z_t, tetragonal). Calcined samples were characterized by means of XRD, UV–vis DRS and FT-IR (using CO and NO as probe molecules).

In Co/Z_m, isolated Co^{2+} anchored to the ZrO_2 surface and small Co_3O_4 particles coexisted. In Co/Z_m, upon exposure to CO at 298 K, isolated Co^{2+} and cobalt ions on the surface of Co_3O_4 easily underwent reduction, yielding Co^{n+}-carbonyls ($n < 2$). Conversely, in sulphated samples, nearly all cobalt was present as isolated Co^{2+}, which was far less reducible with CO at 298 K than isolated Co^{2+} in Co/Z_m. Specifically, the reducibility of isolated Co^{2+}decreased in the order $Co/Z_m > CoS/Z_t > CoS/Z_m \cong Co/Z_mS_g$. On all sulphated samples, surface covalent sulphates formed. The structure of surface covalent sulphates on CoS/Z_t differed from those on CoS/Z_m and Co/Z_mS_g. On Co/Z_mS_g, covalent and ionic sulphates coexisted.

In the temperature range 425–600 K, Co/Z_m samples were poorly active for NO reduction and highly active for NH_3 oxidation. In this temperature range, sulphated samples were inactive for both reactions. They became highly active for NO reduction above 600 K, and for NH_3 oxidation above 675 K. We conclude that the catalytic activity and selectivity of CoO_x/ZrO_2 depend crucially on (i) the presence of isolated Co^{2+} endowed with the proper redox behaviour and (ii) the absence of Co_3O_4.

1. Introduction

The technological, chemical and mechanistic features of the selective catalytic reduction (SCR) of NO_x with NH_3 in the presence of O_2, especially on VO_x-based catalysts, have been reviewed by Bosh and Janssen [1], Busca et al. [2], and, more recently, by Liu et al. [3]. In power plants, a drawback inherent to the SCR process with NH_3 is the SO_2 in the flue gas. On VO_x-based catalysts, in the presence of O_2, SO_2 is oxidized to SO_3. Owing to the concomitant presence of water and unconverted ammonia, SO_3 can give rise to sulphuric acid and ammonium sulphate, resulting in corrosion and deposition of solid by-products downstream from the reactor, where the temperature is lower. To reduce the formation of SO_3 by VO_x, commercial catalysts for SCR are now formulated with WO_x,VO_x/TiO_2 or MoO_x,VO_x/TiO_2 (low VO_x-content) instead of VO_x/TiO_2 (high VO_x-content) [2,4]. Along with the foregoing undesired effects, SO_3 has the advantage of leading to sulphated TiO_2 and sulphated VO_x/TiO_2, which are more active than the parent fresh catalysts for SCR with NH_3 at high temperature [5–11].

Unlike sulphated-TiO_2, sulphated-ZrO_2 (monoclinic or tetragonal) is inactive for SCR. The presence of covalent sulphates does not alone guarantee SCR activity, these species being present in both sulphated-TiO_2 and sulphated-ZrO_2. Active catalysts require the concomitant presence of species possessing redox behaviour, in sulphated-TiO_2, most likely Ti^{IV}/Ti^{III}. Because sulphated-ZrO_2 contains no species endowed with redox behaviour, active ZrO_2-based catalysts require the presence of transition metal ions [2,12]. On CuO_x/ZrO_2 samples, we found that sulphation improved SCR

* Corresponding author. Tel.: +39 06 49913304; fax: +39 06 490324.
E-mail address: daniela.pietrogiacomi@uniroma1.it (D. Pietrogiacomi).

0926-3373/$ – see front matter © 2008 Elsevier B.V. All rights reserved.
doi:10.1016/j.apcatb.2008.11.021

activity with NH_3 [12,13]. The presence of sulphates (i) rendered Cu^{2+} less reducible in sulphated CuO_x/ZrO_2 than in unsulphated ones and (ii) prevented CuO segregation. Because the aforementioned effects reduced the catalytic activity for NH_3 oxidation, in the SCR of NO with NH_3 sulphated samples were more selective than CuO_x/ZrO_2 [12]. The same activity and selectivity results have been obtained in sulphated and in unsulphated CuO_x/ZrO_2 for the SCR of NO with propene [14].

The effect of sulphating CoO_x/ZrO_2 has been previously investigated for the SCR of NO with hydrocarbons [15–17]. When C_3H_6 was used as a reductant, sulphated samples were far more active and selective than the corresponding unsulphated CoO_x/ZrO_2, even though sulphates had a weaker effect on the catalytic performance of samples with Co-content < 2 Co-atoms nm^{-2} [15]. With NH_3 as the reductant, sulphates can induce an analogous effect as recently reported for unsupported Co_3O_4 [18]. All these findings prompted us to investigate the effect of sulphation on CoO_x/ZrO_2 catalysts for SCR with NH_3. Sulphated catalysts, with a Co-content of 2 atoms nm^{-2}, were prepared by two different methods (wet impregnation and *via* gas-phase) and compared with CoO_x/ZrO_2. Because the tetragonal or monoclinic crystalline phase of sulphated-ZrO_2 can determine catalytic behaviour, as it does for the catalytic isomerisation of *n*-butane [19], we were also interested in comparing a sulphated monoclinic sample with a sulphated tetragonal one, having the same cobalt and sulphate surface density. Samples were characterized by XRD, UV–vis DRS, and FT-IR spectroscopy and used as catalysts for the SCR of NO with NH_3 and for the $NH_3 + O_2$ reaction.

2. Experimental

2.1. Catalyst preparation

The zirconia support was prepared by hydrolyzing zirconium oxychloride with ammonia, as already described [20]. The hydrous zirconium precipitate was washed with water until the Cl^- test with $AgNO_3$ gave no visible opalescence. Before its use as support, the material was dried at 383 K for 24 h, Z_{hydr}, and calcined at 823 K for 5 h, Z_m, where m specifies the structure after calcining at 823 K (monoclinic).

Unsulphated cobalt-containing samples were obtained following the same procedure previously adopted [24]. CoO_x/ZrO_2 were prepared by impregnating Z_m with aqueous solutions of $Co(CH_3COO)_2$, drying at 383 K and calcining at 823 K. Samples were labelled $Co/Z_m(x)$, where x specifies the analytical cobalt content (atoms nm^{-2}).

Three cobalt-containing sulphated catalysts, with roughly the same cobalt surface density (2 Co-atoms nm^{-2}) were prepared by two procedures. In the *first procedure* a portion of $Co/Z_m(2.0)$ was sulphated *via* the gas-phase, by exposing it to a stream containing 1000 ppm SO_2 and 36 000 ppm O_2 in He at 673 K (1000 Ncc/min) for 5 h. This sample was labelled $Co/Z_m(2.0)S_g(y)$, where S_g stands for "gas-phase sulphation" and y specifies the analytical sulphate content (molecules nm^{-2}), for short hereafter Co/Z_mS_g. In the *second procedure*, a weighted amount of Z_{hydr} or Z_m was impregnated with an aqueous solution of $CoSO_4$. Samples were thereafter dried at 383 K and calcined at 823 K. The two samples were labelled $CoS/Z_a(x, y)$, where a specifies the crystallographic phase after calcining at 823 K (t, tetragonal or m, monoclinic), x specifies the analytical cobalt content (atoms nm^{-2}) and y the analytical sulphate content (molecules nm^{-2}), for short hereafter CoS/Z_t or CoS/Z_m. Cobalt content was determined by atomic absorption (Varian SpectrAA-30). Sulphate content was determined by extracting sulphates with NaOH 1 M, and ionic chromatography of the resulting solution (Dionex 2000i). Surface areas ($SA/m^2\,g^{-1}$) were measured by N_2 adsorption at 77 K. Samples and their main features are listed in Table 1.

Table 1
Samples and their main features.

Starting material	Sample	Co (wt%)	SO_4 (wt%)	S.A. ($m^2\,g^{-1}$)
$Zr(OH)_4$	Z_{hydr}			
ZrO_2	Z_m			59
$Z_m + Co(CH_3COO)_2$(aq)	$Co/Z_m(2.0)$	1.1		59
$Z_m + Co(CH_3COO)_2$(aq)	$Co/Z_m(4.6)$	2.2		50
$Co/Z_m(2.0) + SO_2 + O_2$ *in situ*	$Co/Z_m(2.0)S_g(1.0)$[a]	1.1	1.0	59
$Z_m + CoSO_4$	$CoS/Z_m(2.0, 1.9)$[b]	1.1	1.8	59
$Z_{hydr} + CoSO_4$	$CoS/Z_t(2.0, 1.8)$[c]	1.7	2.6	91

[a] In the text, for short, Co/Z_mS_g.
[b] In the text, for short, CoS/Z_m.
[c] In the text, for short, CoS/Z_t.

2.2. Characterization techniques

FTIR spectra were recorded at room temperature (RT) on a PerkinElmer 2000 spectrometer equipped with an MCT detector, collecting 100 scans at a resolution of 4 cm^{-1}. Powdered materials were pelleted (pressure 1.5×10^4 kg cm^{-2}) in self-supporting disks of ca. 16 mg cm^{-2} and 0.1–0.2 mm thickness. All samples were placed in an IR quartz cell allowing heating *in vacuo* or in controlled atmosphere. Before experiments, samples were heated in O_2, from RT to 793 K, kept at that temperature for 0.5 h, and evacuated thereafter at the same temperature for 1 h (standard activated samples). Absorbance spectra were obtained by subtracting the relevant background. Spectra after adsorption of gaseous probes are difference spectra.

UV–vis DRS spectra were recorded in air at room temperature, in the wavelength range 200–2500 nm on a Varian Cary 5E spectrophotometer with the diffuse reflectance attachment. Halon was used as reference.

XRD patterns were obtained with a Philips PW 1729 diffractometer (Ni-filtered Cu Kα radiation) equipped with an on-line computer (software APD-Philips).

2.3. Catalytic measurements

Catalysts were tested in a flow apparatus consisting of a feeding section, a reaction section and a gas analysis section. High purity gas mixtures, NO/He, NH_3/He, O_2 and He, were fed through mass flow controllers (Hitech) to a fixed bed microreactor, made of two coaxial quartz tubes (i.d. 35 and 16 mm) to allow preheating of feed gas. The microreactor was heated with an electrical oven (Watlow) driven by a temperature controller (Yokogawa PY 27) allowing about 6 cm isothermal length. A K-type thermocouple monitored the temperature of the catalytic bed. The powder catalyst (0.3 g) was pelleted, crushed and sieved to 180–355 μm. Continuous NDIR analysers were used to measure the concentration of reactants and products: Advance Optima Uras 14 (Hartmann & Braun) for NO and N_2O, Ultramat 5E (Siemens) for NH_3. An on-line gas chromatograph (Dani 86.10 HT) equipped with a TCD detector and a double packed column (Alltech CTR 2) was used for N_2, and O_2 analysis. A P_2O_5 trap avoided interference from the reaction of ammonia with water.

SCR process ($NO + NH_3 + O_2$) was run by feeding a gas mixture containing 700 ppm NO, 700 ppm NH_3, 36 000 ppm O_2, balance He. NH_3 oxidation ($NH_3 + O_2$) was run by feeding a gas mixture containing 700 ppm NH_3, 36 000 ppm O_2, balance He. Before catalysis, the sample was treated in air flow at 823 K for 0.17 h. Catalytic activity was measured in plug flow conditions at steady-state conversion. Space velocity GHSV was about $10^5\,h^{-1}$. In all

catalytic tests, nitrogen balance was at least 95%. In the SCR process, we assumed that all catalysts brought about the following set of reactions:

$$4NO + 4NH_3 + O_2 \rightarrow 4N_2 + 6H_2O \quad (1)$$

$$4NO + 4NH_3 + 3O_2 \rightarrow 4N_2O + 6H_2O \quad (2)$$

$$4NH_3 + 3O_2 \rightarrow 2N_2 + 6H_2O \quad (3)$$

$$4NH_3 + 5O_2 \rightarrow 4NO + 6H_2O \quad (4)$$

$$4NH_3 + 4O_2 \rightarrow 2N_2O + 6H_2O \quad (5)$$

The $NH_3 + O_2$ process caused reactions (3)–(5). Hereafter, we will refer to reactions (1) and (2) as NO reduction, and (3)–(5) as NH_3 oxidation. The percent selectivity in the NO converted compared with the NH_3 converted, S_{SCR}, was calculated as 100 × (NO converted)/(NH_3 converted). The percent N_2O yield in the SCR and in $NH_3 + O_2$ was calculated as 100 × (N_2O produced)/(N_2 inlet), with N_2 inlet corresponding to the concentration of nitrogen-containing reagents fed to the reactor and expressed as equivalent nitrogen: N_2 inlet = (NO inlet) + (NH_3 inlet)/2 or (NH_3 inlet)/2. The percent NO yield in $NH_3 + O_2$ was calculated as 100 × (NO produced)/(NH_3 inlet). The areal rate of NO reduction was determined from NO molecules converted per s per nm^2 in reactions (1) and (2), in experiments yielding <40% conversion.

3. Results and discussion

3.1. XRD and DRS characterization

In all samples prepared from Z_m, XRD pattern disclosed a tetragonal ZrO_2 fraction <10%. In the CoS/Z_t sample prepared from Z_{hydr}, XRD showed the tetragonal ZrO_2 pattern with a small fraction of monoclinic ZrO_2 (<20%). Apparently, impregnating Z_{hydr} with cobalt sulphate stabilised ZrO_2 in the tetragonal phase, in agreement with the analogous stabilisation observed with ammonium sulphate or sulphuric acid [21,22] or copper sulphate [12]. None of the samples showed XRD reflections from Co_3O_4 or $CoSO_4$.

DRS spectra of Co/Z_m samples consisted of bands at 7000, 14,000 and 22,500 cm^{-1}, typical of Co_3O_4 [23,24]. The intensity of Co_3O_4 bands was higher on Co/Z_m(4.6) than on Co/Z_m(2.0) (Fig. 1, spectra 1 and 2). The amount of Co_3O_4 in these samples was determined by means of X-ray photoelectron spectroscopy. XPS spectra (not reported for brevity) were analysed using the same procedure we have previously adopted to determine the Co_3O_4 amount in CoO_x/ZrO_2 samples containing various Co amount, up to about 5 atoms nm^{-2}, as described in details in Ref. [24]. The Co_3O_4 amount in Co/Z_m(2.0) and Co/Z_m(4.6) were 35% and 63%, in that order, the remaining cobalt being present as isolated Co^{2+}.

The comparison of the DRS spectrum of Co/Z_m(2.0) with those of sulphated samples showed that the sulphate presence markedly decreased Co_3O_4 segregation. The band intensity at 14,000 cm^{-1} (typical of Co_3O_4) was much lower in monoclinic CoS/Z_m than in Co/Z_m(2.0), and weak absorptions in the region 21,000–16,000 cm^{-1} appeared (Fig. 1, spectrum 3), and were assigned to Co^{2+} in octahedral sites [25]. The Co_3O_4 band at 14,000 cm^{-1} was absent and the bands of Co^{2+} in octahedral sites were more intense in tetragonal CoS/Z_t than in the CoS/Z_m (Fig. 1, spectrum 4). On the whole, the amount of Co_3O_4 decreased in the order Co/$Z_m \gg$ CoS/$Z_m \geq$ CoS/Z_t, and therefore, that of octahedral Co^{2+} increased in the order Co/$Z_m \ll$ CoS/$Z_m <$ CoS/Z_t.

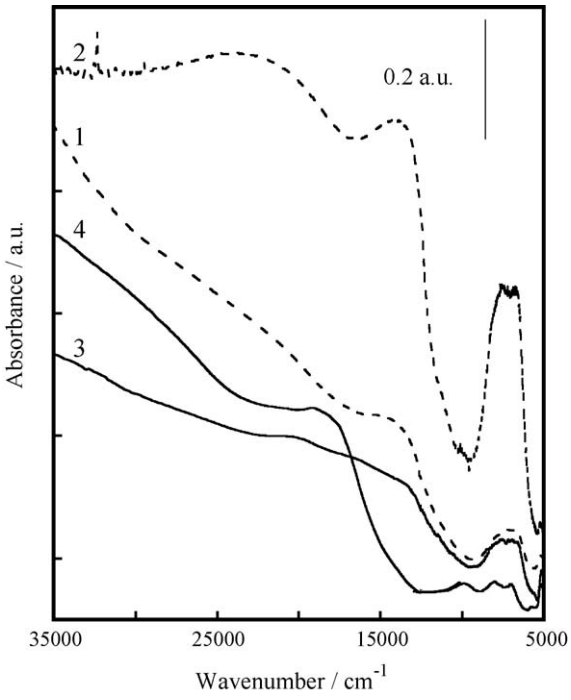

Fig. 1. UV–vis DRS spectra of unsulphated and sulphated CoO_x/ZrO_2. Samples: Co/Z_m(2.0) (spectrum 1), Co/Z_m(4.6) (spectrum 2), CoS/Z_m (spectrum 3), CoS/Z_t (spectrum 4).

3.2. FTIR characterization

3.2.1. Surface sulphates

After evacuation at 793 K, the FTIR spectrum of Co/Z_m(2.0) evidenced weak bands at 3777 and 3673 cm^{-1} (spectrum not shown), assigned to terminal and bridged hydroxyls of the parent Z_m [26]. The intensity of both hydroxyl bands was lower than that on pure ZrO_2. The terminal OH preferentially decreased. We have previously attributed the intensity decrease in the ZrO_2 hydroxyl bands to the Co–O–Zr species formed in the cobalt anchoring process [24]. On sulphated samples, irrespective of the preparation method, OH bands were absent and intense absorptions in the 1400–900 cm^{-1} region appeared, arising from surface sulphates [27]. In particular, the spectrum of CoS/Z_m (Fig. 2, spectrum 1) consisted of several ν_{S-O} bands in the 1250–900 cm^{-1} region and a complex $\nu_{S=O}$ absorption in the 1400–1350 cm^{-1} region, ascribed to tri-dentate covalent sulphates carrying a single S=O oscillator [28,29] and polynuclear sulphates [27]. Similar sulphate bands have been previously observed on monoclinic sulphated-ZrO_2 [27,30] and monoclinic CuO_x-sulphated ZrO_2 [12]. On Co/Z_mS_g, in addition to covalent sulphates, ionic sulphates also formed, as indicated by an intense absorption band in the 1200–1050 cm^{-1} region [31] (Fig. 2, spectrum 2). Ionic sulphates arose from the reaction of segregated Co_3O_4 on the Co/Z_m(2.0) surface with the gaseous stream $SO_2 + O_2$, yielding Co^{2+} SO_4^{2-}.

Compared with monoclinic CoS/Z_m, covalent sulphates of tetragonal CoS/Z_t (Fig. 2, spectrum 3) were somewhat different, consisting of a $\nu_{S=O}$ at about 1380 cm^{-1}, and a less resolved ν_{S-O} absorption in the 1250–950 cm^{-1} region, with a sharp component at about 1040 cm^{-1}. Similar bands have been previously observed on tetragonal sulphated-ZrO_2 [12,19] and assigned to bidentate sulphates possessing two coupled S=O oscillators [19]. As discussed by Morterra et al. [19], the bands of covalent sulphates on monoclinic ZrO_2 differ from those of tetragonal ZrO_2, due to the different geometry of sulphates anchored to different crystal planes.

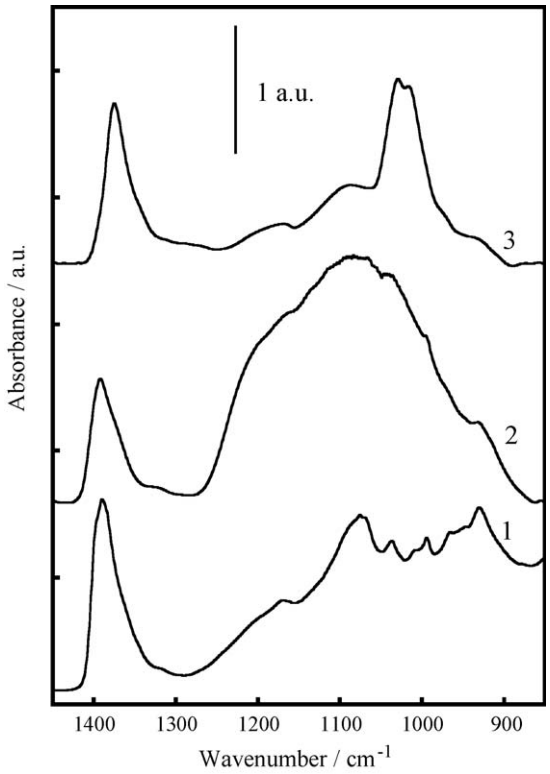

Fig. 2. FTIR spectra of standard activated sulphated samples. Samples: CoS/Z_m (spectrum 1), Co/Z_mS_g (spectrum 2), CoS/Z_t (spectrum 3).

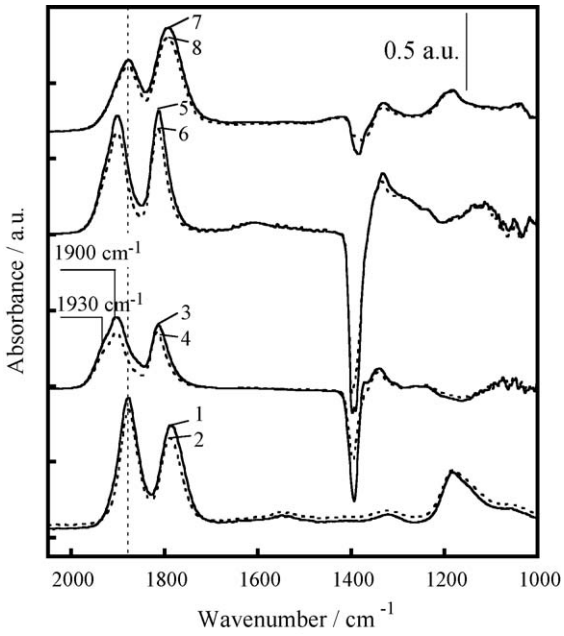

Fig. 3. Difference FTIR-spectra of standard activated samples, after exposure to NO at RT, with p_{NO} = 80 Torr (solid lines) and after NO evacuation at RT for 5 min (dotted lines). Samples: Co/Z_m(2.0) (spectra 1 and 2), Co/Z_mS_g (spectra 3 and 4), CoS/Z_m (spectra 5 and 6) and CoS/Z_t (spectra 7 and 8).

3.2.2. NO adsorption

On Co/Z_m(2.0) sample, the adsorption of NO yielded two intense nitrosyl bands at about 1875 and 1775 cm^{-1} and a broad absorption of nitrites and nitrates in the 1250–1000-cm^{-1} region (Fig. 3, spectrum 1). In agreement with previous assignments [15,32], we assign the nitrosyl band at about 1875 cm^{-1} to Co^{2+}-NO and that at 1775 cm^{-1} to the ν_{asym} of Co^{2+}-$(NO)_2$, whose ν_{sym} partly overlapped the mono-nitrosyl band at 1875 cm^{-1}. In CoO_x/ZrO_2 samples containing isolated Co^{2+} only, we have previously shown that the Co^{2+}-nitrosyl total integrated intensity (cm^{-1}) was proportional to the Co-content [15]. The Co^{2+}-nitrosyl band intensity of Co/Z_m(2.0) fell below this linear correlation, as expected on the basis of UV–vis DRS and XPS analysis for Co_3O_4 in this sample.

On the gas-phase sulphated Co/Z_mS_g, Co^{2+}-nitrosyl bands blue-shifted and partially resolved. In particular, compared with Co/Z_m(2.0), on Co/Z_mS_g, Co^{2+}-NO occurred at 1900 cm^{-1}, the ν_{asym} of the Co^{2+}-$(NO)_2$ occurred at 1815 cm^{-1}, and a distinct shoulder at 1930 cm^{-1} appeared, arising from the ν_{sym} of the Co^{2+}-$(NO)_2$ (Fig. 3, spectrum 3). Owing to the electron withdrawing effect of surface sulphates, the Lewis acid strength of isolated Co^{2+} increased, and hence the wavenumber of nitrosyl bands increased, as previously reported for similar sulphated CoO_x/ZrO_2 samples [15,33]. The Co^{2+}-nitrosyl bands on CoS/Z_m were nearly identical in position and shape to those on Co/Z_mS_g, however more intense (Fig. 3, spectrum 5). Hence, the Lewis acidity of isolated Co^{2+} was identical for the two monoclinic samples, whereas the Co^{2+} surface density was lower on Co/Z_mS_g than on CoS/Z_m, because Co^{2+} SO_4^{2-} segregated in Co/Z_mS_g.

Compared with the CoS/Z_m sample, on the tetragonal CoS/Z_t, Co^{2+}-nitrosyl bands occurred at a lower wavenumber and the dinitrosyl/mono-nytrosyl ratio was higher (Fig. 3, spectrum 7), indicating that the surface morphology affects both the Co^{2+} Lewis acid strength and its coordinative unsaturations.

On all sulphated samples, NO adsorption caused the $\nu_{S=O}$ band to shift toward lower wavenumbers, yielding a negative absorption at about 1400–1350 cm^{-1}, due to side interactions of surface sulphates with adjacent irreversibly adsorbed NO_x species. Because evacuation at RT left nitrosyl and nitrate bands unchanged, this treatment failed to restore the sulphate band to its original position (Fig. 3, spectra 2, 4, 6 and 8). The much lower intensity of the negative peak in CoS/Z_t than in the monoclinic sulphated samples indicated that in CoS/Z_t the side interactions of surface sulphates with adjacent Co^{2+} were weak.

Collectively, NO adsorption evidenced the following order of Co^{2+} Lewis acid strength: $Co/Z_mS_g \simeq CoS/Z_m \gg CoS/Z_t \simeq Co/Z_m$. The weak side interaction of sulphates with adjacent Co^{2+} accounts for the fact that the Lewis acid strength of Co^{2+} on CoS/Z_t nearly equalled that of Co^{2+} on Co/Z_m.

3.2.3. CO adsorption

On Co/Z_m(2.0), CO adsorption at RT yielded several bands of carbonyls in the region 2190–1700 cm^{-1}, and bands of carbonates in the region 1650–1000 cm^{-1} (Fig. 4, spectrum 1). We have previously observed these bands on CoO_x/ZrO_2 samples with various Co-content and we have assigned the components at 2190–2185 cm^{-1} to Zr^{4+}-CO species, those at 2180–2100 cm^{-1} to carbonyls of Co^{3+} and Co^{2+}, and those in the region 2100–1700 cm^{-1} to Co^{n+}-carbonyls ($n < 2$) and to bridged carbonyls [24]. Evacuation at RT completely removed Zr^{4+}-CO, markedly decreased Co^{3+}-CO and Co^{2+}-CO and left all the other bands unchanged (Fig. 4, spectrum 2). The stability of the various carbonyls agreed with the foregoing assignments. Accordingly, the back-donation from the cobalt adsorbing site to CO orbitals, reinforcing site-CO bond, decreases with increasing positive charge on the metal [34]. The concomitant formation of Co^{n+}-carbonyls ($n < 2$) and carbonates indicated a redox process. In our previous study [24], we also clarified that both isolated Co^{2+} and Co-ions on the Co_3O_4 surface underwent reduction upon exposure to CO at RT.

On the gas-phase sulphated Co/Z_mS_g, CO adsorption at RT yielded a band at 2200 cm^{-1}, which markedly decreased on

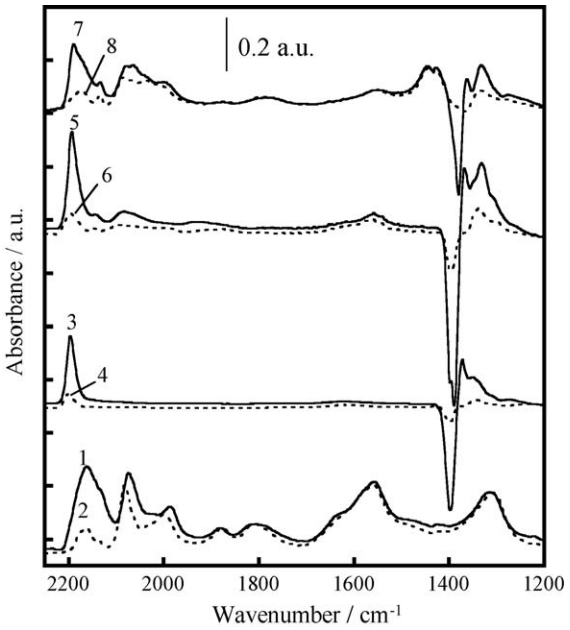

Fig. 4. Difference FTIR-spectra of standard activated samples, after exposure to CO at RT, with p_{CO} = 80 Torr (solid lines), and after CO evacuation at RT for 5 min (dotted lines). Samples: $Co/Z_m(2.0)$ (spectra 1 and 2), Co/Z_mS_g (spectra 3 and 4), CoS/Z_m (spectra 5 and 6) and CoS/Z_t (spectra 7 and 8).

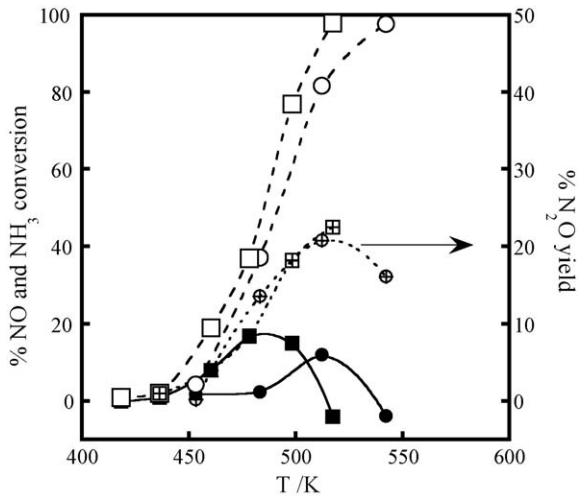

Fig. 5. SCR reaction on Co/Z_m samples. Left axis: percent NO conversion (closed symbols) and percent NH_3 conversion (open symbols) as a function of temperature (T/K). Right axis: percent N_2O yield (crossed symbols) as a function of temperature (T/K). Catalysts: $Co/Z_m(2.0)$ (●, ○, ⊕) and $Co/Z_m(4.6)$ (■, □, ⊞).

evacuation at RT (Fig. 4, spectra 3 and 4). We have previously observed this band on sulphated CoO_x/ZrO_2 samples with various Co-content and we have assigned it to Co^{2+}-CO [15]. The absence of Co^{n+}-carbonyls ($n < 2$) and carbonates indicated that CO did not reduce isolated Co^{2+}, in the presence of covalent sulphates, which withdraw electrons from O^{2-}, thus hampering the reduction of Co^{2+}.

On CoS/Z_m, CO adsorption led to the same results as on Co/Z_mS_g (Fig. 4, spectra 5 and 6). On this sample, however, a very small amount of Co^{n+}-carbonyls ($n < 2$) and carbonates formed, arising from the reduction of cobalt on the surface of Co_3O_4, the latter being present in traces.

On CoS/Z_t, in addition to Co^{2+}-CO, CO adsorption yielded Co^{n+}-carbonyls ($n < 2$) and carbonates (Fig. 4, spectrum 7). On this sample, because Co_3O_4 is absent, Co^{n+}-carbonyls ($n < 2$) arise from the reduction with CO of isolated Co^{2+}. The weak carbonate bands in the 1450–1400 cm^{-1} region were almost identical to those previously observed upon CO_2 adsorption on tetragonal ZrO_2 and assigned to polydentate carbonates [35].

On all sulphated samples, CO adsorption shifted the $\nu_{S=O}$ complex band from about 1400 cm^{-1} to a lower wavenumber, yielding a negative absorption at about 1400–1350 cm^{-1} (Fig. 4). Besides removing labile carbonyls, evacuation at RT almost restored the sulphate bands to their original shape and position (Fig. 4, spectra 4, 6, and 8). Hence, we attributed the $\nu_{S=O}$ shift to side interactions of surface sulphates with nearby carbonyls.

On the whole, the reducibility of isolated Co^{2+}, evaluated from the band intensity of Co^{n+}-carbonyls ($n < 2$), decreased in the order $Co/Z_m > CoS/Z_t > CoS/Z_m \cong Co/Z_mS_g$.

3.3. Catalysis

3.3.1. The catalytic activity of Co/Z_m samples for SCR

In the range 400–600 K, Co/Z_m catalysts were almost inactive for NO reduction. Increasing the reaction temperature caused NO conversion to reach a maximum of hardly 15%, and NH_3 conversion to increase monotonically up to 100%. The temperature of the maximum NO conversion was lower on $Co/Z_m(4.6)$ than on $Co/Z_m(2.0)$. On both catalysts, the N_2O yield reached a maximum of about 20%. In the whole temperature range, NH_3 conversion was higher than NO conversion, indicating that the amount of NH_3 consumed with NO in reactions (1) and (2) was smaller than that consumed with O_2 in reactions (3)–(5) of the SCR process. On both catalysts, the NO conversion became negative above 500 K (Fig. 5). The selectivity S_{SCR} was 50% at 400 K and steeply decreased with temperature, becoming negative above 500 K (vide infra). The negative NO conversion and S_{SCR} values depend on the fact that the amount of NO produced in reaction (4) was higher than that consumed in reactions (1) and (2).

3.3.2. The catalytic activity of Co/Z_m samples for $NH_3 + O_2$

In the same temperature range explored for the SCR reaction, 400–600 K, Co/Z_m catalysts were highly active for the $NH_3 + O_2$ reaction, yielding N_2, NO and N_2O. Increasing the reaction temperature caused NH_3 conversion to increase monotonically. NH_3 conversion, and N_2, NO and N_2O yields were higher on $Co/Z_m(4.6)$ than on $Co/Z_m(2.0)$ (Fig. 6). On $Co/Z_m(2.0)$, the maximum N_2O yield was 10% in the $NH_3 + O_2$ reaction, whereas it was 20% in the SCR, suggesting that N_2O arose from both NO reduction and NH_3 oxidation.

The high activity of Co/Z_m catalysts in the $NH_3 + O_2$ reaction accounts for their low activity for NO conversion and their low S_{SCR} selectivity in the SCR reaction. We assign these unfavourable features to the presence of Co_3O_4 in Co/Z_m catalysts. The finding that the activity of $Co/Z_m(4.6)$ for NH_3 oxidation is higher than that of $Co/Z_m(2.0)$ (Fig. 6) arises from the higher Co_3O_4 amount present in $Co/Z_m(4.6)$ than in $Co/Z_m(2.0)$ catalysts. Other authors have previously reported that unsupported Co_3O_4 [18] and CoO_x/TiO_2 samples containing Co_3O_4 [36] are highly active for NH_3 oxidation and almost inactive for NO reduction.

3.3.3. The effect of sulphation on the activity for SCR and $NH_3 + O_2$

The catalytic activity for SCR of the sulphated samples, Co/Z_mS_g and CoS/Z_m, differed markedly from that of the unsulphated one, $Co/Z_m(2.0)$. Compared with $Co/Z_m(2.0)$, on both Co/Z_mS_g and CoS/Z_m (i) the temperature at which NO and NH_3 started to react was higher, by about 100 K, (ii) NO conversion was much higher, (iii) NH_3 conversion and N_2O yield were lower (Fig. 7). The S_{SCR} selectivity on Co/Z_mS_g and CoS/Z_m was markedly higher than on $Co/Z_m(2.0)$ (Fig. 8).

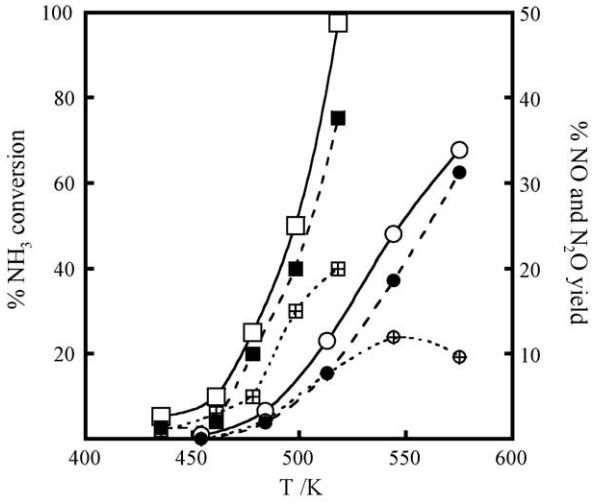

Fig. 6. $NH_3 + O_2$ reaction on Co/Z_m samples. Left axis: percent NH_3 conversion (open symbols) as a function of temperature (T/K). Right axis: percent NO yield (closed symbols) and percent N_2O yield (crossed symbols) as a function of temperature (T/K). Catalysts: $Co/Z_m(2.0)$ (○, ●, ⊕) and $Co/Z_m(4.6)$ (□, ■, ⊞).

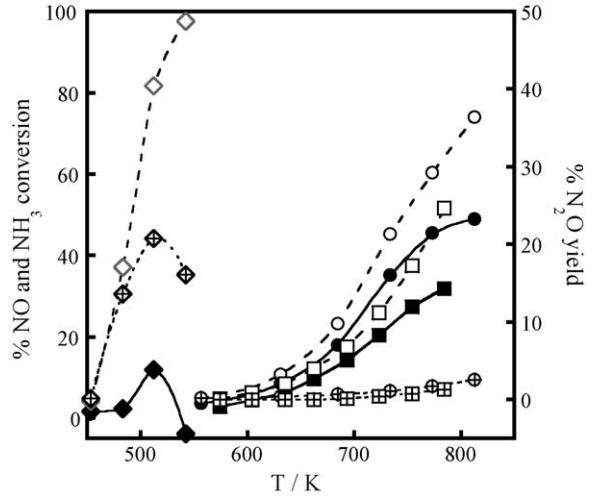

Fig. 7. The effect of sulphation on the SCR reaction. Left axis: percent NO conversion (closed symbols) and percent NH_3 conversion (open symbols) as a function of temperature (T/K). Right axis: percent N_2O yield (crossed symbols) as a function of temperature (T/K). Catalysts: $Co/Z_m(2.0)$ (◆, ◇, ⊕), Co/Z_mS_g (■, □, ⊞), and CoS/Z_m (●, ○, ⊕).

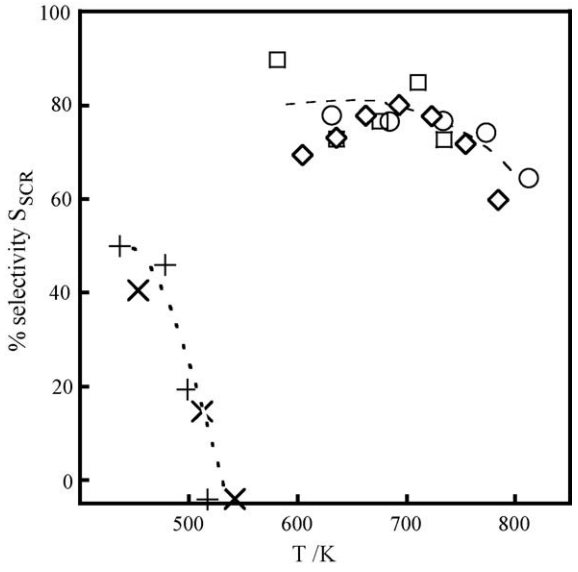

Fig. 8. The effect of sulphation on the selectivity S_{SCR}. Percent selectivity S_{SCR} as a function of temperature (T/K). Catalysts: $Co/Z_m(2.0)$ (+), $Co/Z_m(4.6)$ (×), CoS/Z_m (○),Co/Z_mS_g (◇) and CoS/Z_t (□).

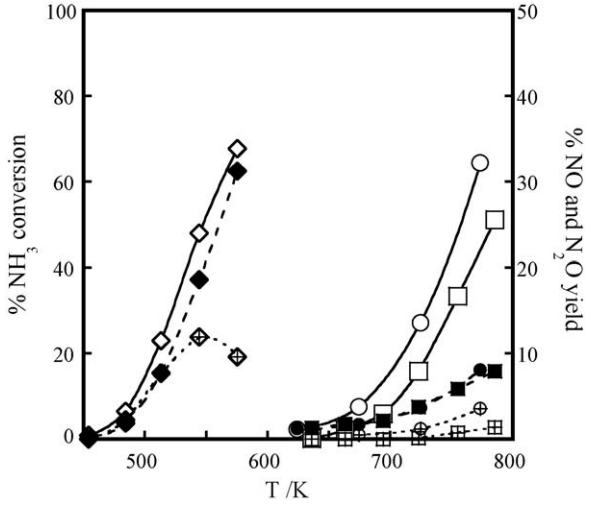

Fig. 9. The effect of sulphation on the $NH_3 + O_2$ reaction. Left axis: percent NH_3 conversion (open symbols) as a function of temperature (T/K). Right axis: percent NO yield (closed symbols) and percent N_2O yield (crossed symbols) as a function of temperature (T/K). Catalysts: $Co/Z_m(2.0)$ (◇, ◆, ⊕), Co/Z_mS_g (□, ■, ⊞), and CoS/Z_m (○, ●, ⊕).

As it did for SCR, the catalytic activity for $NH_3 + O_2$ of Co/Z_mS_g and CoS/Z_m differed markedly from that of $Co/Z_m(2.0)$. Compared with $Co/Z_m(2.0)$, on both Co/Z_mS_g and CoS/Z_m (i) the reaction onset temperature for $NH_3 + O_2$ was higher, by about 200 K, and (ii) the NO and N_2O yields were much lower (Fig. 9).

Whereas on $Co/Z_m(2.0)$ the onset temperature for $NH_3 + O_2$ and that for SCR almost matched, on Co/Z_mS_g and CoS/Z_m the onset temperature for $NH_3 + O_2$ was about 75 K higher than that for SCR (Fig. 10). Hence, the S_{SCR} selectivity was higher for Co/Z_mS_g and CoS/Z_m than for $Co/Z_m(2.0)$ (Fig. 8). Because covalent sulphates stabilised the isolated Co^{2+} oxidation-state, the onset temperatures for both SCR and $NH_3 + O_2$ were higher on Co/Z_mS_g and CoS/Z_m than on $Co/Z_m(2.0)$.

3.3.4. The effect of the sulphation procedure

On the catalyst CoS/Z_m, NO conversion in the SCR and NH_3 conversion in the $NH_3 + O_2$ reaction were higher than on Co/Z_mS_g (Fig. 7). The two catalysts had the same selectivity S_{SCR} (Fig. 8). The higher amount of isolated Co^{2+} in CoS/Z_m than in Co/Z_mS_g accounts for the higher NO and NH_3 conversions. The nearly identical redox properties of isolated Co^{2+} explain why the two samples had identical S_{SCR} selectivity.

3.3.5. The effect of the crystallographic phase: tetragonal versus monoclinic

The sulphated tetragonal CoS/Z_t was highly active for NO reduction (Fig. 11a). In CoS/Z_t, (i) the onset temperature for NO conversion was about 50 K lower, (ii) the maximum NO conversion was substantially higher, and (iii) N_2O yield lower than in the corresponding monoclinic CoS/Z_m, containing the same surface density of both cobalt and sulphate (Fig. 11a). The two samples showed similar selectivity S_{SCR} (Fig. 8). Because the two samples

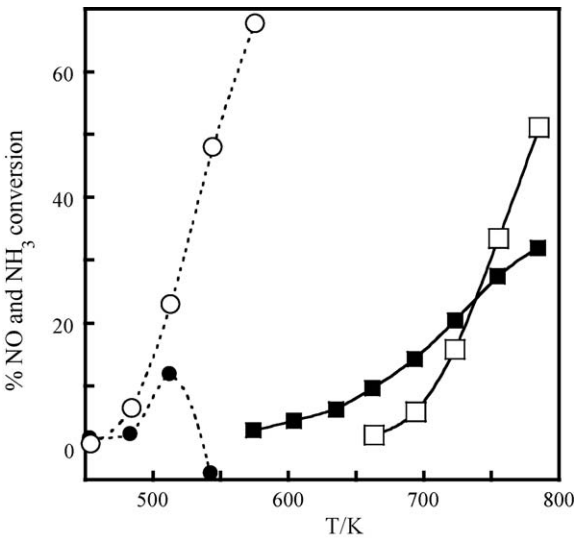

Fig. 10. Percent NO conversion in the SCR reaction (closed symbols) and percent NH_3 conversion in the $NH_3 + O_2$ reaction (open symbols) on $Co/Z_m(2.0)$ (●, ○) and Co/Z_mS_g (■, □), as a function of temperature (T/K).

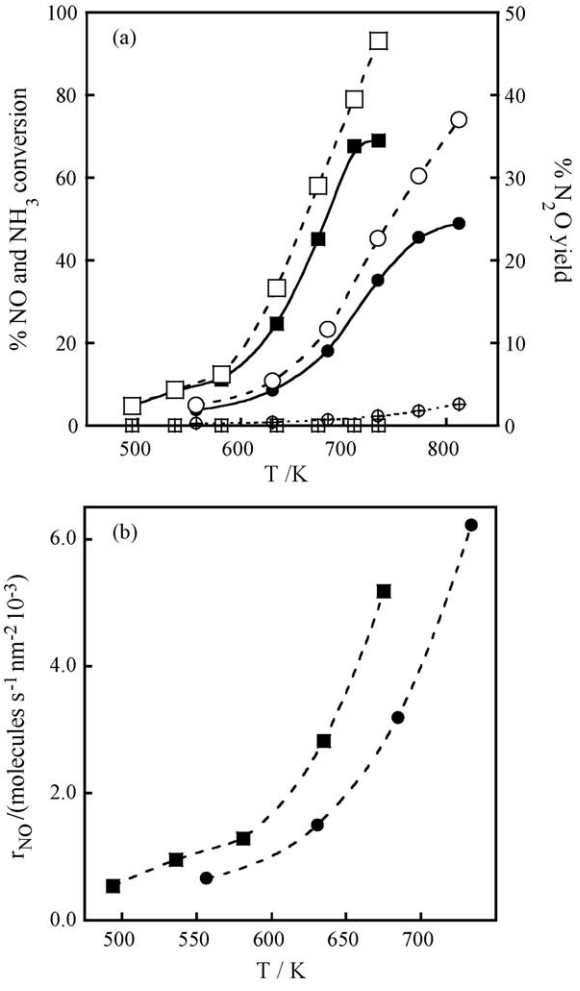

Fig. 11. A comparison between tetragonal and monoclinic sulphated samples. Section a: percent NO conversion (closed symbols, left axis), percent NH_3 conversion (open symbols, left axis) and percent N_2O yield (crossed symbols, right axis) as a function of temperature (T/K) on the monoclinic CoS/Z_m (●, ○, ⊕) and on the tetragonal CoS/Z_t (■, □, ⊞). Section b: areal rate of SCR (r_{NO}/NO molecules converted per nm^2 per second) as a function of temperature (T/K) on the monoclinic CoS/Z_m (●) and on the tetragonal CoS/Z_t (■).

differed substantially in surface area, they are better compared through areal rates of NO reduction (r_{NO}/molecules s^{-1} nm^{-2}), rather than conversions. The areal rate r_{NO} of CoS/Z_t was higher than that of CoS/Z_m (Fig. 11b). The FTIR characterization with CO shows that isolated Co^{2+} is stabilised to a lower extent in CoS/Z_t than in CoS/Z_m. This difference explains why the NO reduction rate was higher for CoS/Z_t than for the CoS/Z_m catalyst.

3.3.6. The effect of the Lewis acid strength

The Lewis acid-strength of Co^{2+} determined by FTIR using NO as a probe molecule affects neither the range of temperature in which catalysts are active nor their selectivity S_{SCR}. Specifically, CoS/Z_t and $Co/Z_m(2.0)$, having nearly the same Lewis acid-strength of isolated Co^{2+}, are active in well distinct temperature regions. Further, CoS/Z_t and CoS/Z_m, having markedly different Lewis acid-strength of isolated Co^{2+}, displace the same selectivity S_{SCR}.

4. Conclusions

The characterization of sulphated and unsulphated CoO_x/ZrO_2 catalysts shows that sulphation and morphology affect the dispersion, redox properties and Lewis acid strength of cobalt. In parallel, the kinetic study of these catalysts shows that sulphation affects their catalytic activity and selectivity.

In both monoclinic and tetragonal samples, covalent sulphates modulate the redox properties of isolated Co^{2+}, and guarantee the absence of Co_3O_4, thus rendering the sulphated catalysts more active and selective than the unsulphated ones. The catalytic activity and selectivity of CoO_x/ZrO_2 depend crucially on the presence of isolated Co^{2+} endowed with the proper redox behaviour and on the absence of Co_3O_4. Conversely, the Lewis acid strength of isolated Co^{2+} affects neither the activity nor the selectivity S_{SCR} of these samples.

References

[1] H. Bosch, F. Janssen, Catal. Today 2 (1988) 369.
[2] G. Busca, L. Lietti, G. Ramis, F. Berti, Appl. Catal. B: Environ. 18 (1998) 1.
[3] Q. Liu, Z. Liu, C. Li, Chin. J. Catal. 27 (2006) 636.
[4] P. Forzatti, Appl. Catal. A: Gen. 222 (2001) 221.
[5] J.P. Chen, R.T. Yang, J. Catal. 139 (1993) 277.
[6] P. Ciambelli, M.E. Fortuna, D. Sannino, A. Baldacci, Catal. Today 29 (1996) 161.
[7] V.I. Pârvulescu, P. Grange, B. Delmon, Catal. Today 46 (1998), 233 (and references therein).
[8] J.P. Chen, R.T. Yang, Appl. Catal. 80 (1992) 135.
[9] M.D. Amiridis, I.E. Wachs, G. Deo, J.-M. Jehng, D.S. Kim, J. Catal. 161 (1996) 2476.
[10] S.M. Jung, P. Grange, Catal. Today 59 (2000) 305.
[11] S.M. Jung, P. Grange, Appl. Catal. B: Environ. 27 (2000) L11.
[12] D. Pietrogiacomi, D. Sannino, A. Magliano, P. Ciambelli, S. Tuti, V. Indovina, Appl. Catal. B: Environ. 36 (2002) 217.
[13] D. Pietrogiacomi, A. Magliano, D. Sannino, M.C. Campa, P. Ciambelli, V. Indovina, Appl. Catal. B: Environ. 60 (2005) 83.
[14] V. Indovina, D. Pietrogiacomi, M.C. Campa, Appl. Catal. B: Environ. 39 (2002) 115.
[15] D. Pietrogiacomi, M.C. Campa, S. Tuti, V. Indovina, Appl. Catal. B: Environ. 41 (2003) 301.
[16] N. Li, A. Wang, J. Tang, X. Wang, D. Liang, T. Zhang, Appl. Catal. B: Environ. 43 (2003) 195.
[17] N. Li, A. Wang, M. Zheng, X. Wang, R. Cheng, T. Zhang, J. Catal. 225 (2004) 307.
[18] R. Ke, J. Li, X. Liang, J. Hao, Catal. Commun. 8 (2007) 2096.
[19] C. Morterra, G. Cerrato, F. Pinna, M. Signoretto, J. Catal. 157 (1995) 109.
[20] A. Cimino, D. Cordischi, S. De Rossi, G. Ferraris, D. Gazzoli, V. Indovina, G. Minelli, M. Occhiuzzi, M. Valigi, J. Catal. 127 (1991) 744.
[21] M. Sarzanini, G. Sacchero, F. Pinna, M. Signoretto, G. Cerrato, C. Morterra, J. Mater. Chem. 5 (2) (1995) 353.
[22] R.A. Comelli, C.R. Vera, J.M. Parera, J. Catal. 151 (1995) 96.
[23] M. Lo Jacono, A. Cimino, G.C.A. Schuit, Gazz. Chim. Ital. 103 (1973) 1281.
[24] D. Pietrogiacomi, S. Tuti, M.C. Campa, V. Indovina, Appl. Catal. B: Environ. 28 (2000) 43.
[25] A.B.P. Lever, Inorganic Electron Spectroscopy, 2nd ed., Elsevier, Amsterdam, 1984.
[26] V. Indovina, M. Occhiuzzi, D. Pietrogiacomi, S. Tuti, J. Phys. Chem. B 103 (1999) 9967.
[27] C. Morterra, G. Cerrato, V. Bolis, Catal. Today 17 (1993) 505.
[28] M. Bensitel, O. Saur, J.-C. Lavallay, B.A. Morrow, Mater. Chem. Phys. 19 (1988) 147.
[29] F. Haase, J. Sauer, J. Am. Chem. Soc. 120 (51) (1998) 13503.

[30] V. Indovina, M.C. Campa, D. Pietrogiacomi, Stud. Surf. Sci. Catal., vol. 130B, Elsevier, Amsterdam, 2000, p. 1439.
[31] K. Nakamoto, Infrared and Raman Spectra of Inorganic Compounds, 3th ed., J. Wiley & Sons Inc. Publ., New York, 1978 (Table III-19), p. 241.
[32] B. Tsyntsarski, V. Avreyska, H. Kolev, Ts. Marinova, D. Klissurski, K. Hadjiivanov, J. Mol. Catal. A: Chem. 193 (2003) 139.
[33] M. Kantcheva, A.S. Vakkasoglu, J. Catal. 223 (2004) 352.
[34] J.E. Bailie, C.H. Rochester, G.J. Hutchings, J. Chem. Soc., Faraday Trans. 93 (13) (1997) 2331.
[35] K. Pokrovski, K.T. Jung, A.T. Bell, Langmuir 17 (2001) 4297.
[36] M. Wallin, S. Forser, P. Thormählen, M. Skoglundh, Ind. Eng. Chem. Res. 43 (2004) 7723.